PROGRAM REPORT

Advanced Technologies for Hypersonic Propulsive, Energetic and Reusable Platforms
Technical Conference and Exposition
{July 30, 2021}

DAMPING OF STRUCTURES UNDER EXTREME MULTI-AXIAL MECHANICAL AND THERMAL LOADS

Karli Katterle
Ohio Northern University
Ada, OH

Dr. Jeffrey Kauffman
University of Central Florida
Orlando, FL

ABSTRACT

When designing structures, it is essential to consider damping in the design process. To predict the damping of a structure, a damping model is needed. There are different damping models already developed, but they are mostly used for mathematical convenience, and these models depend on frequency. In the aerospace industry, structures are exposed to mechanical and thermal loads. An area of focus in the aerospace industry is the design and development of hypersonic structures, and to help with the design of these structures, an accurate damping model is needed. Along with extreme mechanical loads, hypersonic structures undergo extreme thermal loads as well. This paper will help develop a damping model that is dependent on mechanical and thermal loads being applied on a structure. Using a test stand that was created previously and derived equations, the experimental and theoretical relationship between in-plane loads and damping was developed and compared. The results of this study will help determine if the theoretical relationship between in-plane loads and damping is the same as the experimental relationship between in-plane loads and damping.

NOMENCLATURE

A	Amplitude
f	Frequency
ζ	Damping ratio
ω_{mn}	Natural frequency
ω_{mn_0}	Nominal modal frequency
α_{mn}	Modal stiffness ratio
$\frac{\omega_{mn}}{\omega_0}$	Normalized modal frequency
$\frac{\eta_{mn}}{\eta_{EI}}$	Normalized modal loss factor

1. INTRODUCTION

With many advancements in the aerospace industry, new designs and structures are needed. A consideration that needs to be taken when designing structures in aerospace is damping. Some reasons as to why damping needs to be considered in the design process include: reducing dynamic response to avoid deflection or stress, reducing fatigue loads, ensuring aeroelastic stability, and reducing settling times following transients [1].

In the aerospace industry, there is a high demand for composites in aerospace structures instead of metals. Composites have a lot of potential in the aerospace industry because they could have superior mechanical and thermal properties [1]. However, the damping properties of composites is not as well-known as metallic structures [1]. Additionally, aerospace structures encounter thermal, compressive, and tensile loads, which makes predicting and modeling the damping of the material more difficult during the design process.

To apply damping in the design process, an accurate damping model is needed. There are many different damping models already developed, such as the strain-based and motion-based viscous damping model. The main reason these models are used are because of mathematical convenience. However, they have damping be dependent of frequency, which is not accurate. The strain-based and motion-based damping models rarely accurately show the physics underlying the dissipation mechanisms that exist. Another model used in practice is a structural damping model, the hysteretic damping (complex modulus). Compared to the viscous damping models, the complex modulus model was developed to create a damping model that had a weaker dependence on frequency [1]. The complex modulus damping model has been more accurate when applied in practice than the viscous damping models listed above [2]. These damping models have led to a need in developing a more accurate damping model.

In Ref. [3] a viscous rotation-based “Geometric” damping model was further developed. For a simply supported beam, this model yielded a modal damping that is independent of frequency. Building on the viscous rotation-based “Geometric” damping model, Ref. [4] provides some understanding of the energy dissipation mechanisms [4].

In Ref. [2], using various damping models, a simply supported beam with applied loads was studied. It was found that for all the damping models studied, by increasing tensile loads on the beam, the modal damping decreases compared to having no tension applied to the beam, and applying compressive loads increased the modal damping.

The damping models stated above have been able to better represent damping for beams. In aerospace, extreme mechanical and thermal loads are applied to structures. This can make it difficult to model a structure's damping. The goal of this paper is to help develop a damping model that is dependent on the structure's geometry, the mechanical and thermal loads being applied to the structure.

2. MATERIALS AND METHODS

This paper will focus on predicting the relationship between in-plane loads and damping. Previously, a test stand was designed to induce multi-axial loads to a flat plate. The test stand was designed so that the main function was applying compressive or tensile loads in both planar axes of a flat plate. For the initial testing, an aluminum plate with dimensions of 8"x 8" and a thickness of 0.025" was used.

2.1 Theoretical Setup

To predict the relationship between in-plane loads and damping, theoretical equations derived previously were used [5]. The equation that represents the natural frequency can be found in equation 1 [5]:

$$\omega_{mn}^{2} = \frac{D\pi^4}{\rho a^4}(m^2+\mu^2n^2)^2\left(1+\mu^2\frac{\gamma_x {k_x}^2 m^2+\gamma_y {k_y}^2 n^2}{(m^2+\mu^2n^2)^2}\right) \quad (1)$$

where ω_{mn} is the natural frequency, D is the flexural rigidity, a is the plate dimension in the x direction, ρ is the density, m is the mode number in the x direction, n is the mode number in the y direction, µ is the aspect ratio, γ_x is the nondimensional in-plane load in the y direction, and γ_y is the nondimensional in-plane load in the y direction. The nominal modal frequency is the frequency of the plate when no in-plane loads are being applied which can be seen in equation 2 [5]:

$$\omega_{mn_0}^{2} = \frac{D\pi^4}{\rho a^4}(m^2+\mu^2n^2)^2 \quad (2)$$

where ω_{mn_0} is the nominal modal frequency. Taking equations 1 and 2, the modal stiffness ratio was produced. This can be found in equation 3 [5]:

$$\alpha_{mn} = \frac{\omega_{mn}^{2}}{\omega_{mn_0}^{2}} \quad (3)$$

where α_{mn} is the modal stiffness ratio. To predict the relation between in-plane loads and damping using the theoretical equations, nondimensional terms were developed using equations 1-3. The first nondimensional term is the normalized modal frequency which can be seen in equation 4 [2]:

$$\frac{\omega_{mn}}{\omega_0} = \frac{\sqrt{\alpha_{mn}}\,(m^2+\mu^2n^2)}{(1+\mu^2)} \quad (4)$$

where $\frac{\omega_{mn}}{\omega_0}$ is the normalized modal frequency. The next nondimensional term is the normalized modal loss factor seen in equation 5 [2]:

$$\frac{\eta_{mn}}{\eta_{EI}} = \frac{1}{\alpha_{mn}} \quad (5)$$

where $\frac{\eta_{mn}}{\eta_{EI}}$ is the normalized modal loss factor. Using equations 4 and 5, plots are created to help predict the theoretical relation between in-plane loads and damping. In Figure 1, the relationship between the normalized modal frequency and normalized modal loss factor for a square flat plate (aspect ratio equals 1) can be seen.

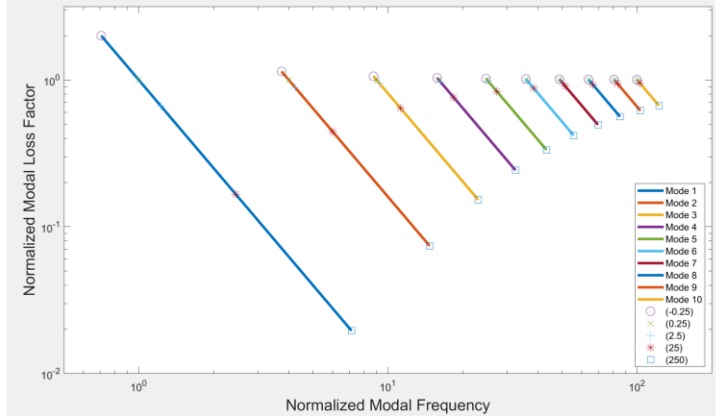

FIGURE 1: Plot of normalized modal frequency and loss factor of the different modes for a square plat.

The different markers on the plot represent an increase in tensile loads. Tensile loads are positive and compressive loads are negative. It can be seen that as the tensile loads increase, the normalized modal frequency increases, and the normalized modal loss factor decreases. Figure 2 shows another plot of the relationship between the normalized modal frequency and loss factor, but with differing in-plane loads, and instead of a square plate with an aspect ratio of 1, the aspect ratio is the golden ratio.

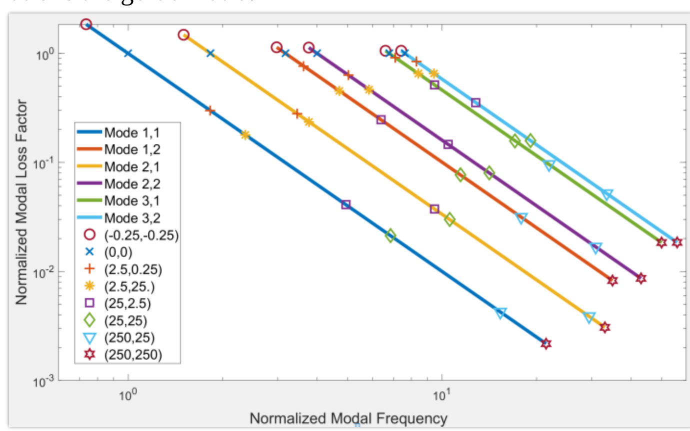

FIGURE 2: Plot of normalized modal frequency and loss factor of the different modes for a plate with an aspect ratio equaling the golden ratio.

In Figure 2, it also shows that as the tensile loads increase, the normalized modal frequency increases, and the normalized modal loss factor decreases.

2.2 Experimental Setup

A flat plate is placed in the test stand and clamped down using four grips. Once the plate is securely clamped in the test stand, compressive loads can be applied. The compressive loads are applied using springs. When the test stand was designed, the springs were chosen to apply compressive loads because it is a simple and inexpensive method to calculate the loads being applied to the plate. Using an impact hammer, an accelerometer, a Data Acquisition Unit, and LabVIEW, data from the test stand is collected. The accelerometer reads the impact from the impact hammer and generates FRF phase and amplitude plots. Using the data from the FRF amplitude plot, the damping ratio is calculated. In Figure 3, the experimental setup of the test stand can be seen.

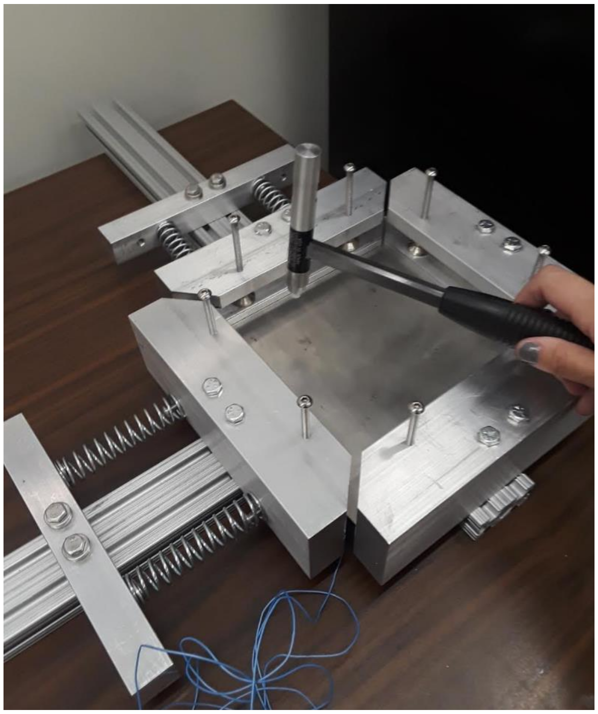

FIGURE 3: Experimental Setup of the Test Stand.

The accelerometer is placed underneath the flat plate and slightly off center, so it can read the impact caused by the hammer. In order to get good readings, the hammer needs to hit the plate in the same location. For each run, the plate is hit with the impact hammer a set number of times with a certain amount of time between each hit. It was found for this research to get the best FRF plots, a test run with 5 hits from the impact with 20 seconds for each hit produced the best results. During each run, the response of each hit is averaged, and from the average an FRF amplitude and phase plot is created.

2.3 Calculating Damping

Using the data collected, the damping of the flat plate in the test stand can be calculated. An FRF plot of the data collected was created using MATLAB. An example of an FRF plot can be seen in Figure 4.

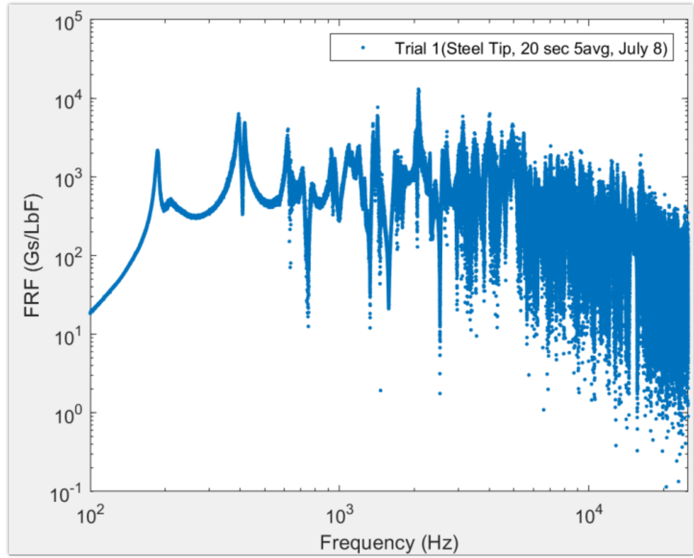

FIGURE 6: FRF amplitude and phase plot from one of the test runs.

Then, using the MATLAB FRF plot and excel the damping was calculated. The method used was the Half-Power Bandwidth method which can be seen in equation 6 [6]:

$$\zeta_r = \frac{f_b - f_a}{2 f_r} \tag{6}$$

where ζ_r is the damping ratio at the natural frequency, f_r is the natural frequency, and f_a and f_b are the frequencies when the amplitude, or response, has half-power of the peak. The power is equivalent to the amplitude squared, so the half-power amplitude is the peak amplitude divided by radical 2. An example of how the needed frequencies were found using the data from the FRF plot can be seen in Figure 5.

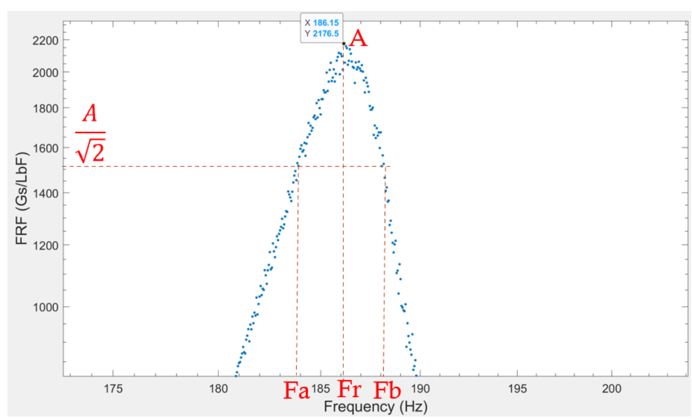

FIGURE 5: Example of a frequency peak used to find the needed frequencies to calculate damping.

The damping ratio is calculated at the different peaks seen on the FRF plot, which represent different modes. The peak's frequency is the natural frequency. The damping ratio is calculated at the peaks that are associated with a phase drop of 180 degrees. This can be found by looking at the FRF phase plot along with the FRF amplitude plot. An example of this can be seen in Figure 6.

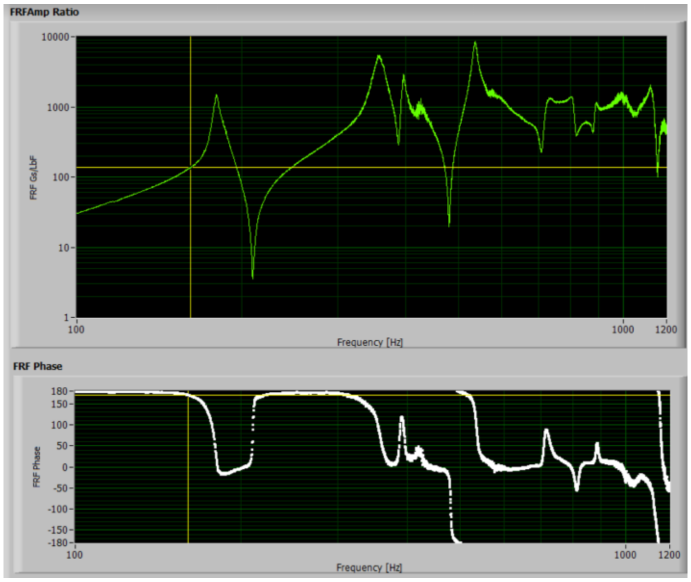

FIGURE 6: FRF amplitude and phase plot from one of the test runs.

For the initial testing, no compressive loads were applied. The initial test was conducted to make sure that the plate secured in the test stand produced the expected calculated damping ratio. To make sure the damping calculated from each test run was consistent, three trials were done. From the initial testing, it was found that the mounted feet on the plate clamps were producing inconsistent results whereas without the mounted feet, the results were consistent. This may be because the mounted feet were adding additional stress to the plate, however that may not be the case. In order to find out, adding a strain gauge to the plate could help determine if additional stress was being added. This could be done for future testing.

2.4 ANSYS

ANSYS was used to simulate flat plates to help compare theoretical and experimental results. The different boundary conditions were simply supported, clamped/fixed, and free. In the theoretical equations, a flat plate with simply supported boundary conditions was simulated in ANSYS to compare the frequency from the equations. When doing the initial testing with no in-plane loads being applied, the boundary conditions of the experimental flat plate were clamped, or fixed. This was also simulated in ANSYS. A plate with free boundary conditions was tested to make sure the experimental setup was correct, and it was also simulated on ANSYS.

It was also used to help visualize the different mode shapes for different boundary conditions of a flat plate. In Figure 7, an example of a simulated flat plate can be seen. The boundary conditions for the plate in Figure 7 are all the sides of the plate are fixed.

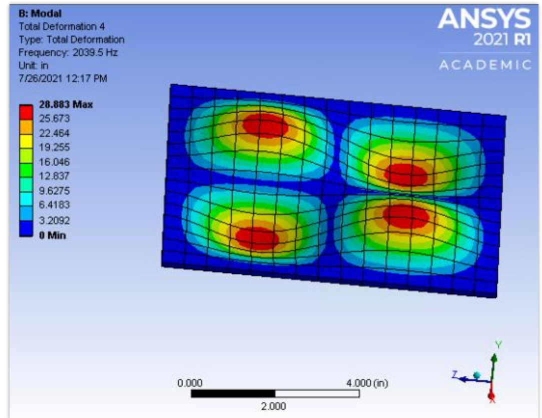

FIGURE 7: Simulated flat plate in ANSYS with fixed boundary conditions.

To make sure the correct peaks were being looked at on the generated FRF plot, the flat plate from the experimental testing was simulated in ANSYS. Table 1 shows and example of comparing the experimental frequency with the frequency found in ANSYS. The data in Table 1 is the percent difference comparing the frequency simulated in ANSYS and the natural frequency of a peak in an FRF plot for a flat plate. The different boundary conditions, clamped, simply supported and free, were all simulated using ANSYS.

Table 1: Frequency comparison of a flat plate

	Frequency (Hz)		
Mode	**ANSYS**	**Experiment**	**Percent Difference**
1	90.73	110	19.20
2	129.96	130	0.0308
3	228.41	220	3.75

3. RESULTS AND DISCUSSION

To determine the experimental relationship between in-plane loads and damping, one compression spring was compressed in increments to slowly increase the compressive load being applied to the plate. For each increment, three test runs were done, so three sets of data were collected for each increment. This was done to make sure the data and calculated damping were consistent.

The predicted relationship between the in-plane loads and damping was that as the compressive load increased, the damping would increase as well. To produce the best results, different boundary conditions of the flat plate were tested. It was found that the best results were produced when only two CT clamps were used. The order of clamping was first the CT clamp that doesn't have a spring being applied to it, then the plate clamps, the spring clamp, and finally, the CT clamp that has the spring applied to it. The spring clamp and the corresponding CT clamp would be released and then clamped again when the spring compressed. The setup for the plate can be seen in Figure 8.

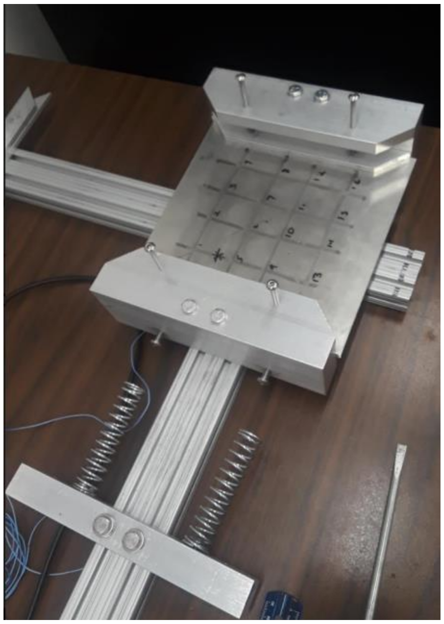

FIGURE 8: Experimental setup of the test stand as spring is compressed.

The damping and frequency were calculated and recorded along with the compressive load being applied to help determine the relationship. In Figure 9, the relationship between the compressive load and frequency can be seen.

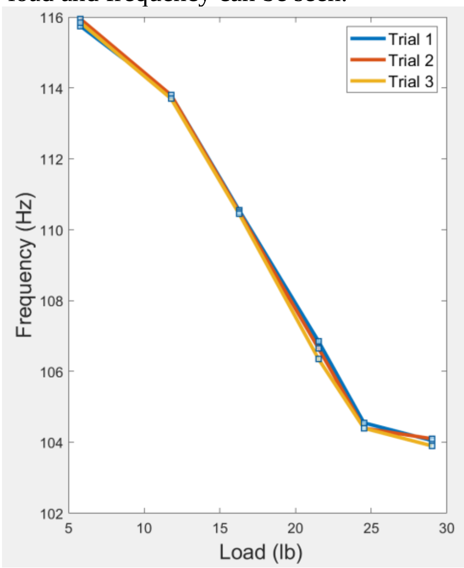

FIGURE 9: Plot of frequency and applied compressive loads.

Looking at Figure 9, it can be seen that as the compressive load increased the frequency decreased. Figure 10 shows the relationship between the compressive load and damping.

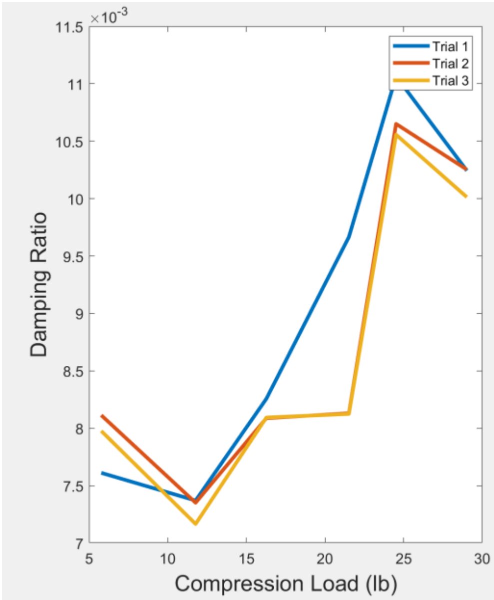

FIGURE 10: Plot of calculated damping and applied compressive loads.

From Figure 10 it can be seen that as the compressive load increases, the damping increases as well. This matches with the expected experimental relationship between the in-plane loads and damping.

To help compare the experimental data with the theoretical data, the relationship between the calculated damping and frequency along with the applied compressive loads needs to be analyzed. Figure 11 shows a plot of the relationship between the calculated damping and the frequency.

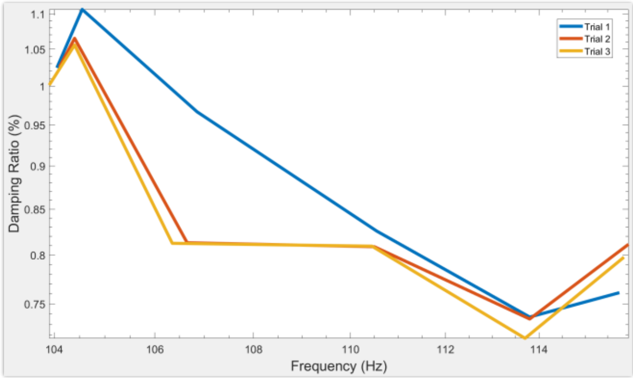

FIGURE 11: Plot of calculated damping and frequency.

In Figure 11, it can be seen that as the frequency increases, the damping decreases. Looking back at Figure 1, it can be seen that this agrees with the theoretical data of the square plate. The theoretical data shows that as the compressive loads increase, the damping increases and the frequency decreases. However, when comparing the experimental and theoretical data and plots, it needs to be considered that the experimental data is on a linear plot, whereas the theoretical data is on a log-log plot. Also, the experimental data collected and presented is equivalent to a very small amount of the theoretical data.

4. CONCLUSION

The initial results confirm the expected in-plane load and damping relationship, however there is still more questions that need to be answered. Some recommendations for future work is to collect data using a stiffer compression spring. This will allow for a bigger compressive load to be applied to the plate. The experimental data will then have a larger range of collected data from in-plane compressive loads, allowing for a better comparison between the experimental and theoretical data.

For this research in-plane loads were applied only in one direction, so another recommendation for future works is to apply loads in the other planar axis. Then a comparison between both directions and the theoretical data can be done. Another recommendation is to apply loads in both planar axes of a flat plate, and vary the loads being applied. This will allow for comparison with the theoretical data found in Figure 2. In the theoretical data, the relationship between damping and tensile loads are also shown, so applying tensile loads on a flat plate will also help compare experimental data with theoretical data. Lastly, another recommendation is to test different materials. For this research, only one material was tested. By testing different materials, it will allow for a better understanding of the relationship between in-plane loads and damping.

ACKNOWLEDGEMENTS

The authors would like to thank Dr. Kauffman for their guidance through the research. Additionally, they would like to thank Christian Vazquez and Chris Kelley for their help during the research.

REFERENCES

[1] Lesieutre, G.,"Damping in Structural Dynamics," in *Encyclopedia of Aerospace Engineering,* R. Blockley and W. Shyy, Eds. 2010, pp. 1-14.

[2] Lesieutre, G., "How Membrane Loads Influence the Modal Damping of Flexural Structures," *AIAA Journal.* July 2009; 47(7): pp. 1642-1646, doi: 10.2514/1.37618

[3] Lesieutre, G., and Kauffman, J., "'Geometric' Viscous Damping Model for Nearly Constant Beam Modal Damping," *AIAA Journal*. July 2013; 51(7): pp. 1688-1694, doi: 10.2514/1.J052174

[4] Kauffman, J., Lesieutre, G., and Babuška, V. "Damping Models for Shear Beams with Applications to Spacecraft Wiring Harnesses," *Journal of Spacecraft and Rockets.* 2014; 51(1): pp. 16-22, doi: 10.2514/1.A32440

[5] Kauffman, J. and Lesieutre, G., Class Lecture, Topic:"How Biaxial Loads Influence the Modal Damping of Flexural Structures." College of Engineering, The Pennsylvania State University, July, 2010.

[6] Kauffman, J., Class Lecture, Topic: "Damping." College of Engineering and Computer Science, University of Central Florida

